ISSN: 2664-9640

Research on Radial Electromagnetic Force of Single Winding BL-BLDC Motor

Xiaowan Tu , Wenshao Bu

Electrical Engineering College, Henan University of Science and Technology, Luoyang 471023, China

Corresponding author: Xiaowan Tu (e-mail: 237837404@qq.com).

Abstract

This paper mainly studies the radial electromagnetic force of single winding bearingless brushless DC (BL-BLDC) motor. First, the electromagnetic relationship inside the motor is analyzed using the equivalent magnetic circuit method, and the mathematical model of the radial electromagnetic force of the motor in the case of a single degree of freedom is derived using the virtual displacement method. The radial electromagnetic force of the motor is composed of the radial magnetic suspension force and the eccentric magnetic pulling force generated by the motor rotor deviating from the center position. Then, the finite element analysis (FEA) software is used to model and simulate the single winding motor, and analyze the change of the magnetic suspension force amplitude under different currents and the influence of different eccentric displacements on the eccentric magnetic pull of the motor. Finally, in order to improve the accuracy of the electromagnetic force mathematical model, compensation coefficients are introduced for the radial suspension force and the eccentric magnetic force. The results show that the theoretical value of the mathematical model after introducing the compensation coefficient is basically the same as the calculation result of FEA, which verifies the correctness and validity of the mathematical model of the radial electromagnetic force of the single winding BL-BLDC motor. It provides a theoretical basis for the precise control of single winding motors.

Keywords

BL-BLDC motor, FEA, mathematical model, radial electromagnetic force, single winding.

1. Introduction

Permanent magnet bearingless brushless DC (BL-BLDC) motor is a new type of magnetic suspension motor that combines bearingless technology and brushless DC motor [1]. With the advantages of no friction, no wear, high speed, long life, etc., it has a wide range of application prospects in the field of high-speed operation [2]. According to the different number of winding groups on the stator teeth, it can be roughly divided into two categories, one is double-winding BL-BLDC motor, the other is single winding BL-BLDC motor. The dual-winding BL-BLDC motor has two sets of windings in the stator slot, one is the torque winding, and the other is the suspension winding, which are used to control the electromagnetic torque of the motor and the magnetic suspension force of the rotor core. If the torque winding and the suspension winding are energized at the same time, serious coupling will occur, which will affect the precise control of the motor. Therefore, solving the coupling problem between the torque winding and the suspension winding is the key to achieving precise motor control [3]. In order to realize the precise control of the motor, the decoupling between the torque and the suspension force must be realized [4-6]. The single winding BL-BLDC motor integrates the torque winding and the suspension force winding, and there is only one set of windings in the stator slot. By setting the

ISSN: 2664-9640

time-sharing conduction law of the winding, it can be used to generate magnetic suspension force and electromagnetic torque when the motor is rotating. The existence of the independent suspension winding reduces the power density of the dual-winding BL-BLDC motor and increases the coupling degree of the magnetic suspension system. The single winding BL-BLDC motor can effectively solve the problems faced by the dual-winding BL-BLDC motor. Therefore, the use of a single winding structure is an inevitable trend in the development of BL-BLDC motors.

M. Ooshima et al. proposed a 12-slot 6-pole single winding BL-BLDC motor structure and its control circuit, and designed an experimental prototype of a single winding BL-BLDC motor controlled by the time-sharing conduction of the torque winding and the suspension winding [7-9]. They used the prototype to carry out the magnetic suspension test of the motor shaft and the acceleration and deceleration experiment of the motor rotor. The experimental results show that the motor rotor can achieve stable suspension, which verifies the effectiveness of the proposed torque winding and suspension force winding time-sharing conduction control scheme. There are few domestic studies on the single winding BL-BLDC motor. This new type of motor only has a set of windings placed in the stator slot, which can be used as the torque winding or the suspension winding. The torque and suspension force are generated according to the rotation of the rotor angular position. Since the windings that generate torque and the windings that generate suspension force are no longer energized with the teeth, the coupling between torque and suspension force will be greatly reduced, making it easier to achieve precise control of the motor [10, 11].

The main purpose of this paper is to derive the mathematical model of the radial electromagnetic force of the single winding BL-BLDC motor, and verify it through the FEA software. Section 2 introduces the structure of the single winding BL-BLDC motor and the composition of the radial electromagnetic force. Section 3 derives the mathematical model of radial electromagnetic force under single degree of freedom. Section 4 introduces the FEA software to verify the radial electromagnetic force mathematical model, and proposes compensation coefficients to optimize the mathematical model. Section 5 presents the conclusions of this paper and the scope of future work.

2. Structure and internal electromagnetic force of the single winding BL-BLDC motor

2.1. Structure of single winding BL-BLDC motor

The single winding permanent magnet BL-BLDC motor studied in this paper is a bearingless motor with an 8/4 topology. The schematic diagram of the motor structure is shown in Fig.1. It uses an outer stator and an inner rotor structure. The inner rotor is composed of a rotor core and 4 tile-shaped permanent magnets. The rotor core is at the inner center of the motor. The permanent magnets are evenly placed on the outer surface of the inner rotor according to the N-S polarity. The outer stator is composed of a stator core, stator teeth, stator slots and stator tooth coils. There are 8 stator teeth evenly distributed on the inner surface of the stator core, a stator slot is distributed between two adjacent stator teeth, and the interval between two adjacent stator slots and two adjacent stator teeth is 45 degrees. The stator windings are composed of 8 stator tooth coils, namely U3, V1, U1, V3, U4, V2, U2, and V4. All windings can be divided into two groups, which are used in turn to generate radial suspension force and electromagnetic torque. One group contains four coils U1, U2, U3, U4, and the other group contains four coils V1, V2, V3, and V4. Each group of coils is independent of each other and is wound on the corresponding stator teeth in turn. According to the change of the angular position of the rotor, the current direction of each group of coils is changed to alternately generate electromagnetic torque and radial suspension force.

ISSN: 2664-9640

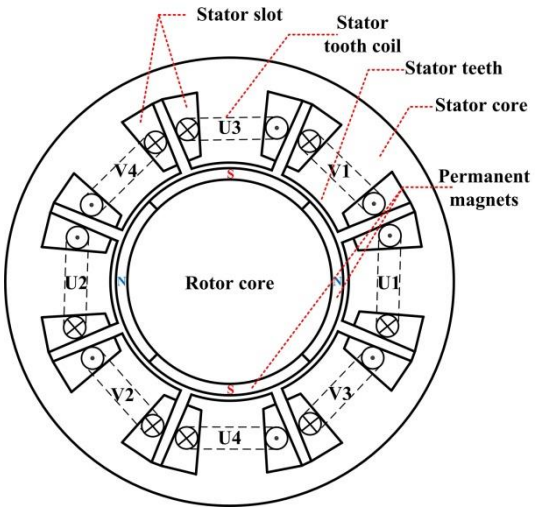

Figure 1: Single winding BL-BLDC motor structure model diagram

2.2. The generation principle of radial electromagnetic force

There are two kinds of forces in the motor. One is the Lorentz force. The force acting on the rotor is mainly along the tangential direction, which is used to control the rotation of the motor. The other is Maxwell's force, its direction is perpendicular to the rotor surface, used to support the rotor suspension. When the magnetic flux distribution of the motor is uniform, the Maxwell force is zero. When the rotor deviates from the axis, the Maxwell force is no longer zero and a force along the eccentric direction of the rotor will appear. The BL-BLDC motor uses this principle to apply excitation to the suspension force winding to break the balance of the original magnetic field. In the air gap magnetic field, the magnetic density on one side is increased, and the magnetic density on the symmetrical side is weakened, thereby generating a suspension force, which will point to the direction of the increased air gap magnetic density. The windings on the two stator slots that are symmetrical about the rotor axis are a pair of suspension force windings, and the two pairs of suspension force windings in the motor are perpendicular to each other, generating two vertical forces. By controlling the magnitude and direction of the current, the magnitude and direction of the force can be controlled, thereby obtaining the bearingless motor with controllable suspension force. Two coordinate planes are defined according to the conduction rule of the suspension force winding as shown in Fig. 2.

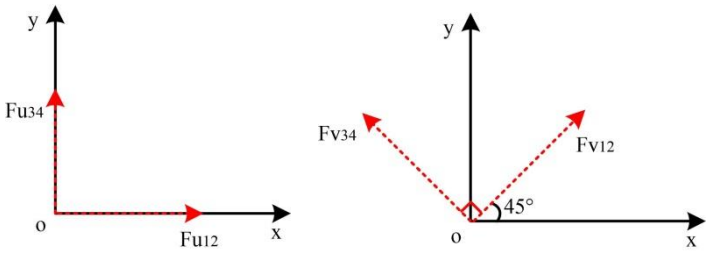

(a) $F_{U12}-F_{U34}$ Coordinate system (b) $F_{V12}-F_{V34}$ Coordinate system

Figure 2: Schematic diagram of the phase of the radial magnetic suspension force generated by a single winding BL-BLDC motor.

The principle of generating radial magnetic suspension force of a single winding BL-BLDC motor is shown in Fig.3. It can be seen that:1) At the current angular position of the rotor, the four magnetic poles of the permanent magnet are facing the coils U1, U2, U3, U4, and the U-phase winding coil is conducive to generating a stable suspension force. Therefore, when the rotor of the motor is in the position shown in the figure, the U phase is used as the floating

ISSN: 2664-9640

winding, and the motor winding coil '•' is the outflow end, and '×' is the current inflow end. According to the right-hand rule, it can be judged that when the rotor of the motor is in the position shown in the figure, the magnetic density of air gap 1 is reduced and the magnetic density of air gap 2 is increased, and radial electromagnetic along the positive direction of the x-axis can be generated inside the motor. 2) In the same way, the magnetic density of air gap 3 is reduced, and the magnetic density of air gap 4 is increased, and radial electromagnetic force along the positive direction of the y-axis can be generated inside the motor.

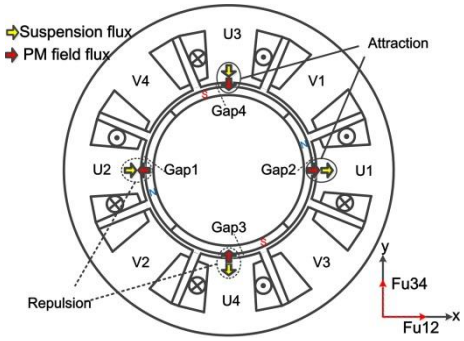

Figure 3: Schematic diagram of suspension force of single winding BL-BLDC motor.

According to the above analysis, it can be seen that by controlling the magnitude of the current excitation applied to the suspension force winding, the magnitude of the radial electromagnetic force in the x-axis direction and the y-axis direction can be controlled, and then the radial suspension force in any direction and size can be obtained. As the position of the rotor changes, the windings that generate the radial suspension force also change. When the rotor just starts to turn out of the U-phase winding, that is, when the rotor rotates to just make the coils V1, V2, V3, and V4 start to face the magnetic poles, the radial suspension force will be generated by the V-phase winding instead.

3. Mathematical modeling of radial electromagnetic force

3.1. Expression of electromagnetic force when the rotor is eccentric

The virtual displacement method has a simple solution process, so it has been widely used in the derivation process of the mechanical model of AC motors. Therefore, this paper also uses this method to derive and calculate the radial electromagnetic force of the motor. The radial electromagnetic force of the BL-BLDC motor includes two parts: the controllable suspension force of the motor and the eccentric magnetic pulling force. For the 8/4 structure single winding BL-BLDC motor, only a single-degree-of-freedom force analysis is carried out, that is, only the suspension force windings U1 and U2 are excited, and the suspension force generated in the motor along the x-axis direction is derived.

In order to facilitate the calculation, the following assumptions were made in the derivation process: 1. Ignore the stator and rotor cogging; 2. Ignore the core leakage flux saturation; 3. Ignore the mutual inductance between the windings; 4. The permanent magnet demagnetization curve and the recovery curve overlap. Assuming that the thickness of the permanent magnet is l_m, the radius of the inner circle of the stator is r, the average air gap length of the motor is δ, the stator pole arc angle is θ_1, the number of turns of the energized winding is N, and the rotor eccentric displacement of the permanent magnet is x. The equivalent magnetic circuit method is used to establish the electromagnetic relationship within the motor. When the current flowing into the U1 winding is i_1, the equivalent magnetic circuit on the U1 side is shown in Fig.4.

ISSN: 2664-9640

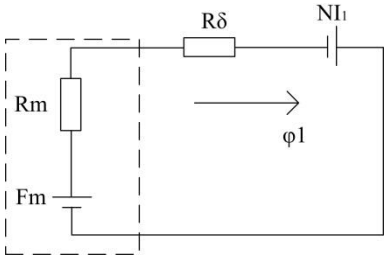

Figure 4: Equivalent magnetic circuit diagram.

In Fig.4, the permanent magnet is equivalent to a constant magnetic flux source, F_{m} is the virtual intrinsic magnetomotive force of the permanent magnet, R_{m} is the reluctance of the permanent magnet, R_{δ} is the air gap reluctance, and φ_1 is the equivalent magnetism The total magnetic flux in the circuit.

According to Ohm's law of the magnetic circuit, the total magnetic flux passing through the magnetic circuit can be expressed as [12]:

$$\varphi_1 = \frac{F_{\mathrm{m}} + Ni_1}{R_{\mathrm{m}} + R_{\delta}} = \frac{N(\frac{F_{\mathrm{m}}}{N} + i_1)}{R_{\mathrm{m}} + R_{\delta}} = \frac{NI_{\mathrm{eq}}}{R_{\mathrm{eq}}} \tag{1}$$

Where, $I_{\mathrm{eq}} = \frac{F_{\mathrm{m}}}{N} + i_1$, $R_{\mathrm{eq}} = R_{\mathrm{m}} + R_{\delta}$, $R_{\mathrm{m}} = \frac{l_{\mathrm{m}}}{\mu_0 S}$, $R_{\delta} = \frac{\delta - x}{\mu_0 S}$, μ_0 is the vacuum permeability, S is the effective magnetic flux area of the magnetic circuit, the calculation formula is:

$$S = \frac{\theta_1}{360^{\circ}} 2\pi r l \tag{2}$$

The virtual intrinsic magnetomotive force of the permanent magnet is expressed as:

$$F_m = H_c l_m = \frac{B_r l_m}{\mu_0 \mu_r} \tag{3}$$

Among them, H_c is the coercive force of the permanent magnet. In the calculation and derivation, set the permanent magnet's recovery permeability μ_r to 1, namely:

$$F_m = \frac{B_r l_m}{\mu_0} \tag{4}$$

According to formula (1), the expression of the total flux linkage in the equivalent magnetic circuit of the permanent magnet is:

$$\psi = N\varphi_1 = \frac{N^2 \mu_0 S\left(\frac{F_m}{N} + i_1\right)}{\delta - x + l_{\mathrm{m}}} \tag{5}$$

Then, the self-inductance of the winding can be expressed as:

$$L = \frac{\mathrm{d}\psi}{\mathrm{d}I_{\mathrm{eq}}} = \frac{N^2 \mu_0 S}{\delta - x + l_{\mathrm{m}}} \tag{6}$$

According to the inductance formula, the expression of electromagnetic energy in the motor can be obtained as follows:

$$W_{\mathrm{m}} = \frac{1}{2} L I_{\mathrm{eq}}^2 = \frac{1}{2} \frac{N^2 \mu_0 S\left(\frac{F_m}{N} + i_1\right)^2}{\delta - x + l_{\mathrm{m}}} \tag{7}$$

ISSN: 2664-9640

Using Newton-Raphson method to expand formula (7), and ignoring its higher-order terms, the following formula can be obtained:

$$W_{\mathrm{m}}=\frac{1}{2}\frac{N^2\mu_0 S\left(\frac{F_m}{N}+i_1\right)^2}{\left(\delta+l_{\mathrm{m}}\right)}\left[1+\frac{x}{\delta+l_{\mathrm{m}}}+\left(\frac{x}{\delta+l_{\mathrm{m}}}\right)^2\right] \tag{8}$$

From formula (8), the electromagnetic force in the motor can be obtained as:

$$F=\frac{\partial W_{\mathrm{m}}}{\partial x}=\frac{1}{2}\frac{N^2\mu_0 S\left(\frac{F_m}{N}+i_1\right)^2}{\left(\delta+l_{\mathrm{m}}\right)}\left[\frac{1}{\delta+l_{\mathrm{m}}}+\frac{x}{\left(\delta+l_{\mathrm{m}}\right)^2}\right] \tag{9}$$

3.2. Expression of controllable magnetic suspension force

The suspension force of the motor is generated by the interaction between the magnetic field generated by the suspension winding and the air gap magnetic field generated by the permanent magnet. Therefore, the magnitude of the suspension force is related to the current value loaded by the winding, and has nothing to do with the eccentricity of the rotor. The motor's suspension force expression does not consider the magnetic pulling force generated by the rotor due to eccentricity. Therefore, the suspension force generated by the energization of the suspension force winding U1 is the term that has nothing to do with x in the electromagnetic force expression, which is recorded as F_1. The suspension force generated by the U2 winding energized has a magnetomotive force opposite to that of the U1 winding, and the suspension force generated by it is recorded as F_2.

From the electromagnetic force expression (9), it can be seen that the suspension force generated by energizing the suspension force winding U1 is:

$$F_1=\frac{1}{2}\frac{N^2\mu_0 S\left(\frac{F_m}{N}+i_1\right)^2}{\left(\delta+l_{\mathrm{m}}\right)^2} \tag{10}$$

The suspension force generated by the U2 winding energized is:

$$F_2=\frac{1}{2}\frac{N^2\mu_0 S\left(\frac{F_m}{N}-i_1\right)^2}{\left(\delta+l_{\mathrm{m}}\right)^2} \tag{11}$$

Therefore, the resultant force of the suspension force along the x-axis direction is:

$$F_u=F_1-F_2=\frac{2SB_{\mathrm{r}}l_{\mathrm{m}}N}{\left(l_{\mathrm{m}}+\delta\right)^2}i_1 \tag{12}$$

It can be seen from equation (12) that when the physical structure of the motor is constant, the magnitude of the suspension force and the magnitude of the current are proportional and linear.

3.3. The mathematical expression of eccentric magnetic pulling force

When the rotor of the motor has an eccentric displacement x in the horizontal direction, an eccentric magnetic pulling force will be generated inside the motor. From equation (9), it can be seen that the U1 winding will produce an eccentric magnetic pulling force along the positive x-axis on the rotor, which is expressed as:

ISSN: 2664-9640

$$F_1 = \frac{N^2 \mu_0 S \left(\frac{F_m}{N}\right)^2}{\left(l_m + \delta\right)^3} x = \frac{B_r^2 l_m^2 S}{\mu_0 \left(l_m + \delta\right)^3} x \tag{13}$$

The eccentric magnetic pulling force generated by the U2 winding on the rotor along the negative direction of the x-axis is:

$$F_2 = -\frac{N^2 \mu_0 S \left(\frac{F_m}{N}\right)^2}{\left(l_m + \delta\right)^3} x = -\frac{B_r^2 l_m^2 S}{\mu_0 \left(l_m + \delta\right)^3} x \tag{14}$$

Therefore, the resultant force of the eccentric magnetic pulling force acting on the rotor produced by the stator windings U1 and U2 is:

$$F_{12} = \frac{2N^2 \mu_0 S \left(\frac{F_m}{N}\right)^2}{\left(l_m + \delta\right)^3} x = \frac{2B_r^2 l_m^2 S}{\mu_0 \left(l_m + \delta\right)^3} x \tag{15}$$

When the motor rotor is eccentric in the x-axis direction, the air gaps corresponding to the U3 and U4 windings in the vertical direction remain basically unchanged, and the eccentric magnetic pulling force in the y-axis direction can be ignored. The air gaps corresponding to the U1 and U2 windings change, and the air gaps corresponding to the V1, V2, V3, and V4 windings also change. These stator windings have a powerful effect on the rotor. Therefore, when the V-phase winding is taken into account, the total eccentric magnetic pulling force that the rotor bears is:

$$F_x = \frac{2B_r^2 l_m^2 S}{\mu_0 \left(l_m + \delta\right)^3} (1 + 2\cos^2 45^\circ) x = \frac{4B_r^2 l_m^2 S}{\mu_0 \left(l_m + \delta\right)^3} x \tag{16}$$

It can be seen from equation (16) that the first and second terms of the polynomial correspond to the eccentric magnetic pull of the U1 and U2 windings and the V-phase winding to the rotor, respectively. Since the offset of the rotor along the y-axis is not considered, the eccentric magnetic pulling force of U3 and U4 is zero. In addition, the eccentric magnetic pulling force of the motor rotor has nothing to do with the current value applied by the stator windings, but only related to the eccentric position of the motor rotor. As the eccentric position of the rotor increases, the amplitude of the eccentric magnetic pulling force will increase proportionally.

3.4. Mathematical model of radial electromagnetic force

The electromagnetic force received by the motor in the horizontal direction is the resultant force of the suspension force and the eccentric magnetic pull force, which can be expressed as:

$$F = F_u + F_x = \frac{2SB_r l_m N}{\left(l_m + \delta\right)^2} i_1 + \frac{4B_r^2 l_m^2 S}{\mu_0 \left(l_m + \delta\right)^3} x \tag{17}$$

The above formula can be written as:

$$F = F_u + F_x = K_u i_1 + K_x x \tag{18}$$

Among them, K_u is the current stiffness coefficient, and K_x is the displacement stiffness coefficient.

4. Simulation of suspension force and eccentric magnetic pulling force

In this section, FEA software is used to verify the radial suspension force and eccentric magnetic pull mathematical model of the single winding BL-BLDC motor. When the rotor is not eccentric,

ISSN: 2664-9640

only the two windings U1 and U2 along the x-axis are supplied with varying current excitation, and the applied current excitation varies from 5 ampere-turns to 50 ampere-turns in steps of 5 ampere-turns. The FEA software is used to calculate the radial suspension force amplitude along the x-axis as shown in Fig.5.

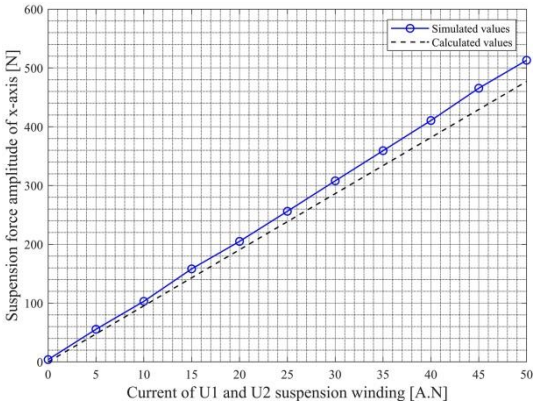

Figure 5: Simulation and calculation values of motor suspension force before correction.

It can be seen from Fig.5 that as the current excitation increases, the suspension force also increases, and when the magnetic circuit is not saturated, the size of the magnetic suspension force basically changes linearly with the excitation current. Therefore, when the magnetic circuit is not saturated, the linearly increasing current will be excited to obtain the same substantially linearly increasing radial magnetic suspension force. It can also be seen from Fig.5 that although there is a certain error between the slope of the radial suspension force calculated by the FEA software and the slope of the change of the magnetic suspension force mathematical model calculation results, the trend or law of change between them is basically consistent. The stiffness coefficient of the suspension force calculated by the mathematical formula is 9.54, and the slope coefficient of the suspension force obtained by the simulation is 10.18. The graph after coefficient compensation is shown in Fig.6, and the model correction coefficient is 1.067.

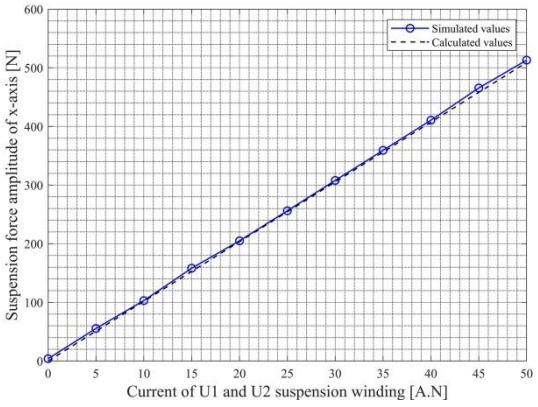

Figure 6: Simulation and calculation values of motor suspension force after correction.

When the eccentric magnetic pulling force of the rotor along the x-axis eccentric position is simulated, the magnetic field generated by the suspension winding current and torque current of the bearingless motor is much weaker than that of the permanent magnet of the rotor. Therefore, no excitation is applied to the suspension force winding, and only the radial electromagnetic force generated by the permanent magnetic field of the rotor when the rotor is eccentric is considered. Select several points from the rotor eccentricity 0.05mm~0.45mm, and take the rotor eccentricity 0.05mm as the step length of each experiment. The experimental results are shown in Fig.7.

ISSN: 2664-9640

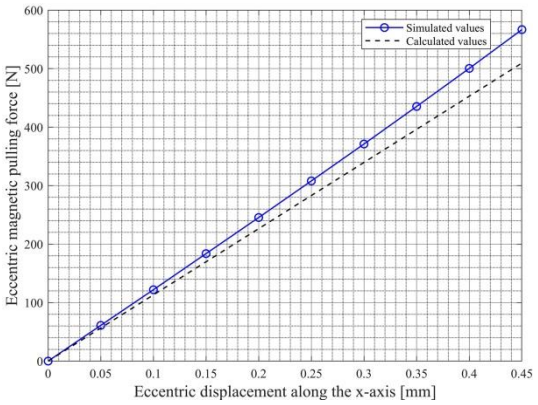

Figure 7: The simulated and calculated values of the eccentric magnetic tension before correction.

It can be seen from Fig.7 that as the rotor displacement of the motor increases, the eccentric magnetic pulling force of the motor basically increases in proportion. At the same time, it can also be found that the simulated value of the eccentric magnetic pull caused by the eccentric displacement of the rotor and the theoretical value derived from the mathematical formula cannot be completely fitted. This is because when the rotor is eccentric, not only the stator teeth are eccentric to the rotor and the magnetic pulling force is generated, but there is also the magnetic pulling force generated by the iron core in other regions to the rotor. However, the influence of this part of the electromagnetic force was ignored in the process of formula derivation. Therefore, the slope of the eccentric magnetic pull obtained by the finite element simulation experiment cannot completely coincide with the slope obtained by the formula derivation.

Therefore, a correction coefficient is introduced to correct the calculated value of the eccentric magnetic pull with the eccentric displacement calculated by the mathematical model, as shown in Fig.8. After adding an appropriate correction coefficient to the model, the simulated value is basically fitted with the calculated value of the mathematical model, and the correction coefficient of the introduced eccentric magnetic tension formula is taken as 1.1. This verifies the validity of the mathematical model of the eccentric magnetic pull caused by the eccentric displacement of the rotor.

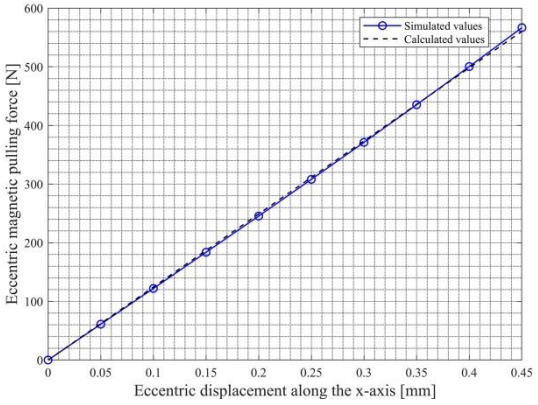

Figure 8: The simulated and calculated values of the eccentric magnetic tension after correction.

5. Conclusion

In order to overcome the shortcomings of the traditional dual-winding BL-BLDC motor, this paper has improved the motor structure. A single winding BL-BLDC motor is proposed and the principle of generating eccentric magnetic pulling force and controllable suspension force is analyzed. In addition, the mathematical model of eccentric magnetic pulling force and

ISSN: 2664-9640

controllable suspension force is established by the virtual displacement method, and the single winding BL-BLDC motor is modeled and simulated by FEA software. By comparison, it can be seen that there is a certain error between the FEA calculation result and the calculation value of the mathematical model. In order to eliminate errors, corresponding compensation coefficients are introduced into the mathematical models of the controllable suspension force and the eccentric magnetic force. After introducing the compensation coefficient, the FEA calculation result is basically the same as the calculation value of the mathematical model, which provides help for realizing the precise control of the motor. In future work, we will study solutions to reduce the coupling between the suspension winding and the torque winding of the single winding BL-BLDC motor.

Acknowledgements

The support of Key scientific and technological projects in Henan Province(202102210095) is acknowledged.

References

[1] Severson E. L.. Bearingless Motor Technology for Industrial and Transportation Applications[C]. 2018 IEEE Transportation Electrification Conference and Expo (ITEC), 2018: 266-273.
[2] Bu W , Huang S , Wan S , et al. General Analytical Models of Inductance Matrices of Four-Pole Bearingless Motors With Two-Pole Controlling Windings. IEEE T MAGN, 14, 7 (2009)
[3] Bu W , Lu P , Lu C , et al. Independent Inverse System Decoupling Control Strategy of Bearingless Induction Motor. Recent Advances in Electrical & Electronic Engineering, 13, 7 (2020)
[4] Bu W , Huang Y , Lu C , et al. Unbalanced displacement LMS extraction algorithm and vibration control of a bearingless induction motor. INT J APPL ELECTROM, 56, 1 (2017)
[5] Bu W , Tu X , Lu C , et al. Adaptive feedforward vibration compensation control strategy of bearingless induction motor. INT J APPL ELECTROM, 63, 2 (2020)
[6] Ooshima M.,Miyashita K.,Rahman M. A.. Control circuit topology of a time-divided torque and suspension force control type bearingless motor[C]. 2012 IEEE Power and Energy Society General Meeting, 2012: 1-4.
[7] Ooshima M.,Miyashita K.,Nakagawa M.. Magnetic levitation tests of a time-divided torque and suspension force control type bearingless motor[C]. 2012 15th International Conference on Electrical Machines and Systems (ICEMS), 2013: 1-6.
[8] Miyashita K.,Ooshima M.,Uddin M. N.. Design of a time-divided torque and suspension force control type bearingless motor[C]. 2011 IEEE Power and Energy Society General Meeting, 2011: 1-4.
[9] Ooshima M.. Winding Arrangement to Increase Suspension Force in Bearingless Motors with Brushless DC Structure[C]. IECON 2007 - 33rd Annual Conference of the IEEE Industrial Electronics Society, 2007: 181-186.
[10] J. Zhu, Z. Q. Deng, X. L. Wang and Q. X. Liao, Principle and Implementation of the Single Winding Bearingless Permanent Magnetic Slice Motor, Proceedings of the CSEE, 28, 33 (2008)
[11] L. G. Chen and H. Q. Zhu, An Accurate Mathematical Model of Radial Suspension Force in Bearingless Brushless DC Motors, Proceedings of the CSEE, 32, 6 (2012)
[12] Chen L, Zhu H . An Accurate Mathematical Model of Radial Suspension Force in Bearingless Brushless DC Motors[J]. Proceedings of the CSEE, 2012.